BMC Medical Genomics

RESEARCH

Open Access

Single cell RNA sequencing provides novel cellular transcriptional profiles and underlying pathogenesis of presbycusis

Juhong Zhang[1], Lili Xiang[2], Wenfang Sun[1], Menglong Feng[1], Zhiji Chen[1], Hailan Mo[1], Haizhu Ma[1], Li Yang[1], Shaojing Kuang[1], Yaqin Hu[1], Jialin Guo[1], Yijun Li[1] and Wei Yuan[1*]

Abstract

Age-related hearing loss (ARHL) or presbycusis is associated with irreversible progressive damage in the inner ear, where the sound is transduced into electrical signal; but the detailed mechanism remains unclear. Here, we sought to determine the potential molecular mechanism involved in the pathogeneses of ARHL with bioinformatics methods. A single-cell transcriptome sequencing study was performed on the cochlear samples from young and aged mice. Detection of identified cell type marker allowed us to screen 18 transcriptional clusters, including myeloid cells, epithelial cells, B cells, endothelial cells, fibroblasts, T cells, inner pillar cells, neurons, inner phalangeal cells, and red blood cells. Cell-cell communications were analyzed between young and aged cochlear tissue samples by using the latest integration algorithms Cellchat. A total of 56 differentially expressed genes were screened between the two groups. Functional enrichment analysis showed these genes were mainly involved in immune, oxidative stress, apoptosis, and metabolic processes. The expression levels of crucial genes in cochlear tissues were further verified by immunohistochemistry. Overall, this study provides new theoretical support for the development of clinical therapeutic drugs.

Keywords Presbycusis, scRNA-seq, Differentially expressed genes, Cochlea

Introduction

Age-related hearing loss (ARHL) or presbycusis is characterized by progressive hearing loss and is often accompanied by poor speech discrimination. A recent systematic review suggests hearing loss affects an estimated 1.57 billion people worldwide, accounting for one in five people, and 2.45 billion individuals will suffer hearing loss by 2050 [1, 2]. The prevalence of hearing loss rises across all age-specific categories, particularly those aged 60 and up to over 80% in adults aged 85 years [3]. As a constellation of sensorineural dysfunctions, ARHL can cause depression, social isolation, and cognitive decline, leading to a severely reduced quality of life [4]. ARHL is a multifactorial condition and is influenced by various internal and external factors, including aging, exposure to noise and ototoxic drugs, genetics, and epigenetic variables [5, 6]. The major sites of cochlear pathology are associated with inner hair cells (HCs), outer HCs, spiral ganglion neurons, and stria vascularis. For example, BNIP3L/NIX is involved in the regulation of cochlear hair cell homeostasis through mitophagy and oxidative stress in ARHL

*Correspondence:
Wei Yuan
yuanwei@ucas.ac.cn
[1]Department of Otorhinolaryngology Head and Neck Surgery, Chongqing General Hospital, No.118, Xingguang Avenue, Liangjiang New Area, Chongqing 401147, China
[2]Department of Otorhinolaryngology Head and Neck Surgery and Hearing Screening and Diagnosis Center, Jinan Maternity and Child Care Hospital, Jinan, Shandong, China

[7]. Oxidative stress can induce premature senescence in auditory cells, leading to ARHL [8]. Meanwhile, the role of immune inflammation in the pathogenesis of presbycusis has also attracted people's attention [9]. However, the biological and pathological mechanisms of ARHL are complex and not yet fully delineated.

Inner ear is a complex structure located in the temporal bone and cochlea is the main sound receiver in the inner ear. Meanwhile, the hair cells and spiral ganglion cells are major structures of sound transmission in the cochlea [10]. Recently, single-cell RNA sequencing (scRNA-seq) technology has been used to define cellular transcriptional data with significant heterogeneity in tissue and organ. Kolla et al. present a scRNA-seq analysis for the cochlear epithelium developing at differential embryonic and postnatal time points; the validation results provides a reliable resource for detecting developmental events during the cochlear formation [11]. Paul et al. demonstrate novel insights into hearing biology according to scRNA-seq of inner and outer hair cells from differential developmental stages, promoting the cell type-defining genes associated with deafness [12].

In this study, we set out to detect the transcriptional heterogeneity of cochlear cell type between young and aged mice. The alteration of cell-cell communications in both young and aged group was analyzed with CellChat, a novel algorithm that can infer cellular communications with scRNA-seq profiles [13]. Moreover, we identified differentially expressed genes (DEGs) associated with presbycusis, followed by functional analysis and immunohistochemical verification. Our data may shed new light on the potential role of cochlea intercellular communications in presbycusis.

Materials and methods

Experimental model

Male C57BL/6J mice were obtained from the Experimental Animal Center of Chongqing Medical University and were divided into two groups, control group (1–2 months old, $n=3$) and aged group (14 months old, $n=3$). All mice were maintained under a low-noise conditions in a 12:12 h light-dark cycle. None of the mice had experienced exposure of noise, otitis media, or ototoxic drugs. The animals were euthanized and cochlear samples were quickly dissected from both ears and submitted to following detection. All experimental procedures were approved by the Laboratory Animal Welfare and Ethics Committee of the Third Military Medical University (ID: IACUC-CQMU-2022-0030).

Auditory brainstem response (ABR) audiometry

ABR tests were performed using a Tucker-Davis Technology equipment as previously described [14]. The mice were anesthetized by intraperitoneal injection of sodium pentobarbital (30 mg/kg), and warmed with a heating pad for maintaining temperature. The recording electrodes were placed in the middle of skull. Reference electrode was inserted subcutaneously behind the ear, while the ground wire was inserted subcutaneously at the tail base. The impedance between the electrodes was less than 3KΩ. The loudspeaker was placed in the external auditory canal, and the ABR threshold was set as the lowest intensity at which the repeatable ABR waveform was identified. The neuronal activity was amplified, filtered, and then digitized with the analog-to-digital converter (AD3; Tucker-Davis Technologies, Alachua, USA). The stimulation pattern used had a rise time of 5 milliseconds and a plateau time of 0.5 milliseconds. The persistence index was detected for 1,000-ms as the ratio of response amplitude at the four frequencies: 8, 16, 24, and 32 kHz. The intensity of the stimuli ranged from 20 to 90 dB sound pressure level (SPL) in 5 dB increments. Three mice with 6 ears were tested.

Single cell RNA sequencing on 10x chromium genomics platform

The mice were euthanized by carbon dioxide to dissect the cochlea and was transported into the iced DMEM (Thermo Fisher Scientific, Waltham, MA) immediately. The stapes, vessels and connective tissues around the cochlea were removed gently under a dissecting microscope. Cochlea was carefully peeled off with dissecting forceps, and the cochlea shaft was removed. Microdissection was completed in 6 cochlear tissues from 3 mice in each group. One biological replicate in each group was used for scRNA-seq. After being washed with the PBS for three times, cochlear tissues were minced into <1 mm^3 size and transferred into a 50 ml tube (BD Falcon, Franklin Lakes, NJ) containing DMEM supplement. Briefly, harvested cochlear tissues were digested with 0.2% collagenase type I for 20 min and then digested with 0.25% trypsin for 10 min. All cells were passed through 40 μm strainers and centrifuged at 300 g at 4 °C for 6 min. The cell pellet was harvested and re-suspended in iced DMEM prior to barcoding on the chromium genomics platform.

The cell counts and cell viability of single cell suspension was measured by Countess II Automated Cell Counter (Thermo Fisher Scientific). The cell viability larger than 85% was adjusted to a concentration of 700–1200 cells/μL and loaded onto the Chromium Controller (10x Genomics, CA, USA). RNA-Seq libraries were prepared using the Chromium Single Cell 5' Reagent Kit v2 (10x Genomics, CA, USA) according to the manufacturer's instructions. The library was constructed for high-throughput sequencing and the reads were subsequently processed using the CellRanger pipeline. Finally, the Cellranger aggr was used to aggregate multiple libraries.

Sequencing data processing

The raw fastq data were mapped to reference genome and quantitated by identifying cellular barcodes using CellRanger [13] (10× Genomics, v3). The quality control criteria were as follows: firstly, the harvested cells outside 2 standard deviations (SDs) from the mean unique molecular identifier (UMI) gene number were filtered out for each sample to discard low-quality cells and doublets. Moreover, the low-quality cells (>10% mitochondrial genes) were further excluded. Doublet analysis was conducted using the DoubletFinder [15] (v2). Finally, a total of 15,401 single cells were acquired.

Seurat clustering

Principal component analysis (PCA) was performed for dimensionality reduction. Clustering results were demonstrated by uniform manifold approximation and project (UMAP). Marker genes were calculated using the function "FindAllMarkers" [16]. The definition of a marker gene is that the gene is highly expressed in the vast majority of the given cell population and lowly expressed in other cell types and the gene is significantly up-regulated in one cell cluster relative to other cell clusters. The specific marker genes of each cell cluster were identified by presto test based on the criteria that the expression proportion of the given cluster was greater than 25% and its expression was higher than that of other clusters. The top 10 marker genes of each cluster were identified based on gene_diff, which was calculated by pct1/pct2. The pct1 was the proportion of cells expressing marker gene in the given cell cluster and pct2 was the proportion of cells expressing marker gene in other cell culsters. Marker gene expression was visualized using VlnPlot and FeaturePlot functions. Cluster annotation was performed using the SingleR [17] package, which compares the transcriptome of single cell to reference datasets that enabled the sub-clustering.

Differential gene identification and enrichment analysis

DEGs between control and aged groups were screened by FindMarkers function in Seurat package based on the criteria of adjusted p-value<0.05 and fold change>1.5. The cell-type specific DEGs were screened based on the criteria of p-value<0.05 and fold change>1.5. Kyoto Encyclopedia of Genes and Genomes (KEGG) enrichment analyses were performed based on hypergeometric distribution test.

Cell-cell communication

Intercellular communication networks perturbed or induced in the cochlear organ were inferred using CellChat1.0.0 [13]. The overall interaction number and interaction strength in differential cell types were quantified and compared between control and disease conditions. The information flows for each signaling pathway were calculated. Finally, to determine the major senders and receivers in the signaling network, cell-cell communications among these seven cell types, were analyzed and compared respectively.

Immunohistochemistry

The cochlear explants ($n=5$) were fixed in 4% paraformaldehyde for 24 h and decalcified with ethylenediaminetetraacetic acid (EDTA) for one month. Then, the cochlear samples were dehydrated by graded alcohol and embedded in paraffin for immunohistochemistry. Cochlear tissue sections were sliced at a thickness of 4–5 μm. After dewaxing, rehydration, and antigen retrieval, the sections were added dropwise with goat serum for endogenous peroxidase blocking. The cochlear tissues were incubated with the primary antibodies including Autotaxin (Enpp2) antibody 1:25; SAA3 antibody 1:50; GH antibody 1:200; RANTES antibody (CCL5) 1:100; CXCL10 antibody 1:100 overnight at 4 °C. Primary antibodies were decanted in PBS and detected using horseradish enzyme-conjugated goat anti-rabbit IgG II (H+L, 1:1000). All images were captured using a confocal microscope (Leica, Heidelberg, Germany).

Results

Identification of major cochlear cell clusters associated with presbycusis

Firstly, the aged mice with severe hearing loss were assessed by ABR threshold assay. Auditory stimuli were applied to mice, and frequency-modulated tones ranging of 8–32 kHz were conducted to test hearing threshold as defined. The median ABR threshold in the aged group was notably elevated compared with the young group mice (Fig. 1A). No hearing was detected in aged mice even at the upper limit of 90dB SPL.

The cellular heterogeneity in presbycusis-related cochlear tissue was evaluated by analyzing mRNA transcripts of the two groups of mice. After filtering the low-quality cells, a total of 10,966 cells were obtained, including 5165 cells in the sample of control group and 5801 cells in the sample of aged group. The average number of UMIs in each cell was ranged from 3636 to 4282 and the average number of genes in each cell was between 879 and 1021. After dimensionality reduction clustering, each single cell was unambiguously assigned to a distinct cluster. A total of 18 optimal cell clusters were visualized by UMAP based on shared nearest neighbor clustering algorithm (Fig. 1B). The distribution differences of the 18 clusters between the two groups is displayed in Fig. 1C and D. The cell numbers of clusters 1, 3, 6, 10, 11, 16 and 18 in the aged mice accounted for more than 50% of all cells in the corresponding clusters. Cell cluster 15, which

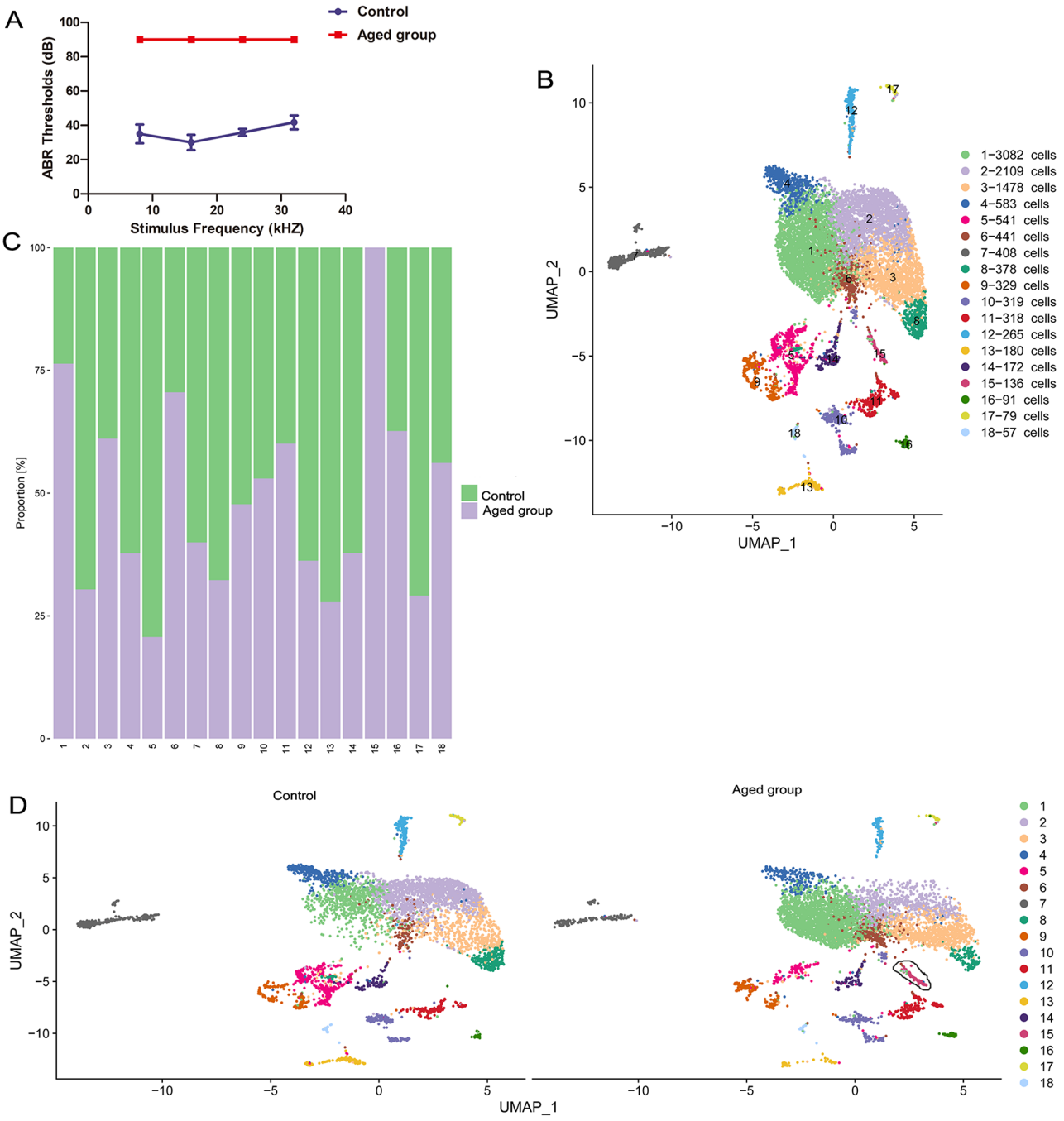

Fig. 1 Identification of crucial cochlear cell types between control and aged mice. (**A**) Hearing threshold of C57BL/6J mice in control and aged group. Frequency dependent stimulus was applied to evaluate the ABR threshold in two groups. $n = 3$ mice/6 ears. (**B**) Uniform Manifold Approximation and Projection plot visualized the single cell clustering colored by different cell types. Each color represents one cluster. (**C**, **D**) The distribution of cells derived from different sample origins. The cell cluster 15 is circled by a black circle

included 136 cells, only appeared in the cochlea of aged mice (Fig. 1D).

Subsequently, the 18 cell clusters were annotated by FindAllMarkers and Single R with well-established marker genes. The heatmap of top 10 marker genes of each cluster is shown in Fig. 2 and the detail information of these marker genes is displayed in Supplementary Table 1. For example, *Fcrla*, *Spib*, *Gm30211*, and *Pax5* were the top marker genes of B cells. *Ncmap*, *Fam178b*, *Pllp*, and *Cldn19* were the top marker genes of inner pillar cells. *Wnt6*, *Kcna6*, *Slc35f1*, and *Cadm2* were the top marker genes of inner phalangeal cells. The cell cluster 15 mainly expressed *Ecrg4*, *Igfbp2*, *Folr1*, and other top marker genes (Supplementary Fig. 1), which can be

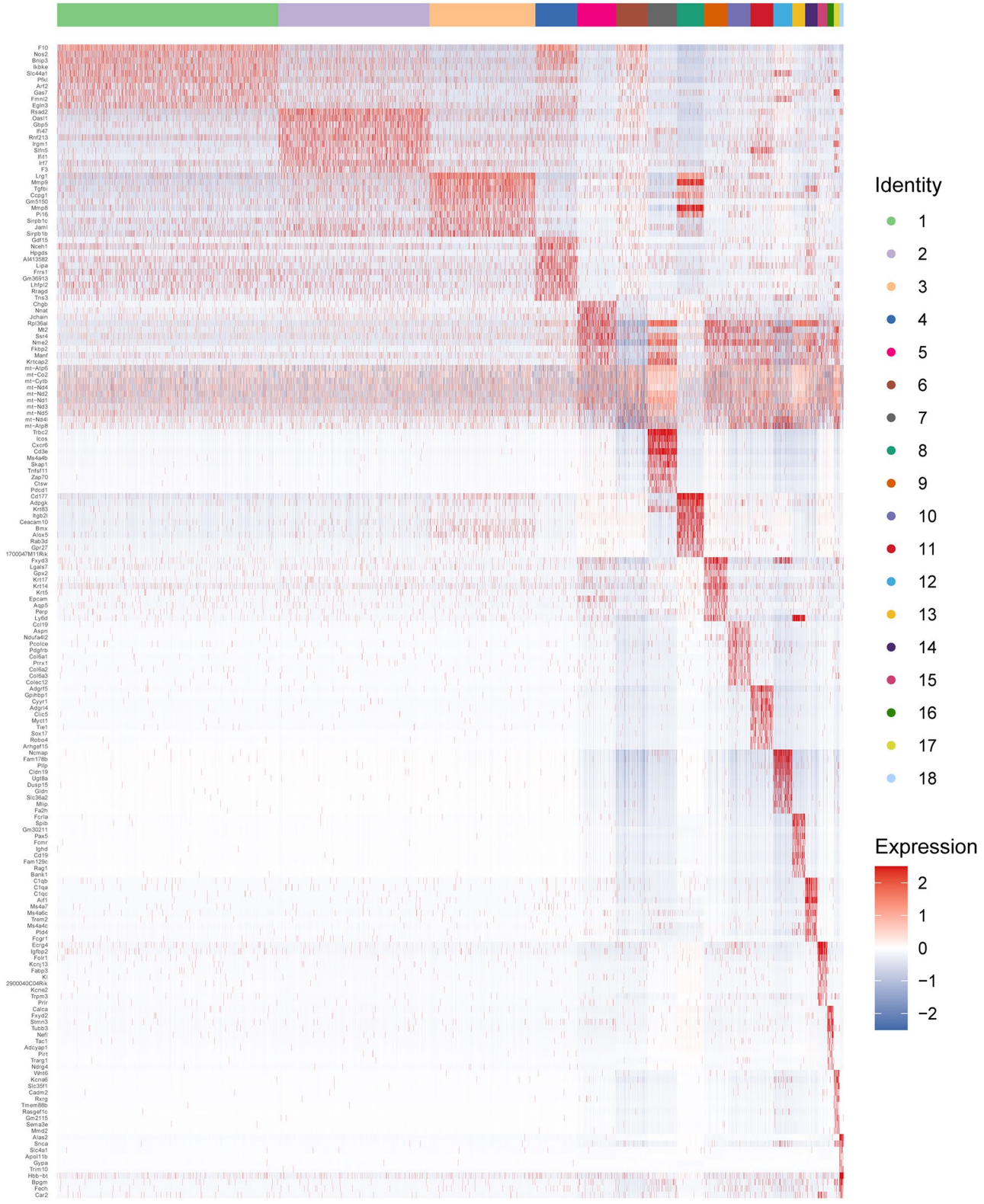

Fig. 2 The heatmap of the top ten marker genes in the 18 clusters. The X-axis is cell cluster, and the Y-axis is marker genes. Red indicates high expression and blue indicates low expression

involved in the regulation of various biological processes such as immunity and metabolism.

Unique gene expression signatures of cochlear subclusters in presbycusis

Annotation of these 18 clusters by marker genes resulted in 10 cell types, including myeloid cells, epithelial cells, B cells, endothelial cells, fibroblasts, T cells, inner pillar, inner phalangeal cells, neurons, and red blood cells (Fig. 3A). Eight distinct clusters of myeloid cells were identified, including cell clusters 1, 2, 3, 4, 6, 8, 14, and 15. Besides, combined with the dataset analysis and the marker genes selection reports in the previous literatures [18–20], clusters 5 and 9 were annotated to be epithelial cells, and both of them showed a decreased number in the cochlea of aged mice. Cells identified as myeloid cells and epithelial cells belong to multiple clusters, suggesting that these cell types were heterogeneous. In addition, although both clusters 5 and 9 were epithelial cells, their top marker gene expression was different. In addition, the counts of epithelial cells, inner pillar cells, inner phalangeal cells, T and B cells were decreased in the cochlear tissues of aged mice, while the counts of endothelial cells, neurons, fibrocytes, and red blood cells were increased in the aged samples (Fig. 3B).

Differential expression analysis

To investigate the DEGs involved in the pathogenesis of presbycusis, we compared the genetic changes between young and aged mice and summarized the most representative signal pathways and biological processes for specific DEG enrichment. A total of 56 DEGs were screened from the aged cochlear tissue comparing with young samples according to the criteria of adjusted p-value < 0.05 (Table 1). Moreover, the DEGs were arranged by the fold change values, and the top 20 significant up- or down- regulated genes were visualized in the heatmap (Fig. 4A). Gene expression status was distinguishable between aged and young cochlear tissues. KEGG functional enrichment showed that the DEGs were mainly involved in "Toll-like receptor signaling pathway", "Cytosolic DNA-sensing pathway", "Leukocyte transendothelial migration", "apoptosis", "Chemokine signaling pathway", "TNF signaling pathway", "Rap1 signaling pathway" and "IL-17 signaling pathway" (Table 2).

Moreover, the cell-type specific gene expression changes were also analyzed between aged and young mice. A total of 119 DEGs were found in the epithelial cells of aged mice, of which 49 genes were up-regulated and 70 genes were down-regulated. A total of 38 DEGs were found in T cells, including 19 up-regulated and 19 down-regulated. There were 113 DEGs in inner pillar cells, including 52 up-regulated and 61 down-regulated. Meanwhile, a total of 242 DEGs were found in the inner phalangeal cells, including 105 up-regulated and 137 down-regulated. A total of 99 DEGs were screened from the endothelial cells, including 29 up-regulated and 70 down-regulated (Supplementary Table 2). VENN analysis of these DEGs showed that Ttr, Prl, Gh and Lyz2 were differentially expressed in all the five cell types (Fig. 4B).

KEGG enrichment analysis of the cell-type specific DEGs showed that the DEGs in epithelial cells were significantly associated with "TNF signaling pathway", "IL-17 signaling pathway", the DEGs in T cells were significantly associated with "cytokine-cytokine receptor interaction", the DEGs in inner pillar cells were significantly associated with "TNF signaling pathway", "Necroptosis", "cellular senescence" and "c-type lectin receptor

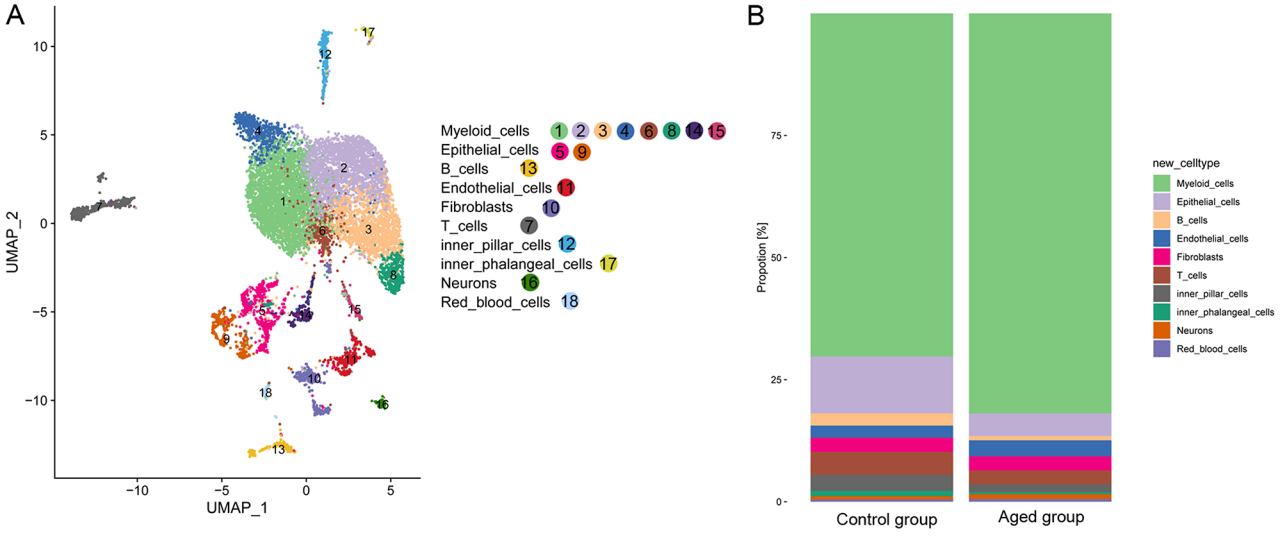

Fig. 3 Annotation of cell clusters. (**A**). Annotated cell types of the single cell clusters. (**B**). Histogram of the cellular proportions between samples from the two groups

Table 1 The list of 56 differentially expressed genes (DEGs) between control and aged mice

Gene	log2FoldChange	pct.1	pct.2	Adjusted *p* value	up_down
Ttr	5.947147	0.858	0	0	Up
Enpp2	1.578948	0.131	0.014	2.06E-113	Up
Saa3	1.222451	0.209	0.123	4.72E-30	Up
AA467197	1.130854	0.524	0.426	5.83E-55	Up
Ezr	1.016209	0.554	0.433	6.27E-91	Up
Hp	0.98054	0.55	0.445	1.63E-46	Up
Ptgds	0.915369	0.079	0.014	1.28E-52	Up
Igha	0.848544	0.166	0.268	3.04E-29	Up
Dleu2	0.82105	0.368	0.245	6.57E-60	Up
Ecrg4	0.797965	0.046	0.01	5.62E-25	Up
Metrnl	0.664096	0.361	0.263	2.30E-40	Up
F10	0.648745	0.434	0.333	2.01E-34	Up
Adgre5	0.644576	0.381	0.255	1.50E-60	Up
Klf7	0.624054	0.343	0.223	8.10E-54	Up
Arf2	0.614509	0.181	0.064	4.75E-76	Up
Ptprc	0.613506	0.697	0.618	5.78E-72	Up
Pirb	0.600321	0.419	0.302	6.80E-54	Up
Prok2	0.599512	0.135	0.11	0.01429558	Up
Rsad2	-0.58511	0.208	0.328	1.85E-41	Down
Rps19	-0.59166	0.4	0.56	8.12E-60	Down
Rps3a1	-0.5974	0.566	0.685	1.03E-45	Down
Rplp0	-0.60073	0.549	0.696	6.08E-66	Down
Cd79b	-0.61089	0.012	0.04	5.46E-16	Down
Vpreb3	-0.61896	0.007	0.03	4.61E-16	Down
Rps26	-0.61918	0.436	0.585	4.36E-56	Down
Rpl11	-0.62553	0.453	0.6	2.73E-58	Down
Rps15a	-0.62899	0.469	0.617	1.83E-59	Down
Rpsa	-0.63224	0.348	0.51	1.72E-61	Down
Igkc	-0.64055	0.639	0.908	2.17E-290	Down
Iglc1	-0.66116	0.01	0.049	3.51E-31	Down
Rpl32	-0.66735	0.39	0.552	3.10E-64	Down
Ly6d	-0.67319	0.031	0.061	2.43E-10	Down
Mpo	-0.68997	0.016	0.054	3.04E-23	Down
Ighg2c	-0.71001	0.143	0.351	6.68E-130	Down
Pmp22	-0.75201	0.038	0.078	1.11E-14	Down
Meg3	-0.78168	0.012	0.076	4.76E-58	Down
Ighm	-0.82914	0.041	0.082	8.37E-16	Down
Tmsb10	-0.86771	0.198	0.345	1.36E-65	Down
Cxcl10	-0.87352	0.159	0.274	2.22E-45	Down
Mt2	-0.87523	0.097	0.252	6.19E-95	Down
Prtn3	-0.88596	0.026	0.077	7.18E-30	Down
Ccl5	-0.90421	0.018	0.049	8.44E-15	Down
Isg15	-0.92526	0.371	0.529	1.05E-77	Down
Mpz	-0.99276	0.038	0.084	4.55E-20	Down
Lipf	-1.00726	0.376	0.61	2.10E-108	Down
Chgb	-1.0778	0.001	0.09	1.16E-113	Down
Sbpl	-1.1338	0.324	0.372	0.02656102	Down
Wfdc18	-1.18211	0.434	0.509	1.42E-06	Down
Mt1	-1.18981	0.217	0.466	2.26E-154	Down
Ifi27l2a	-1.35522	0.149	0.406	3.87E-205	Down
Elane	-1.36648	0.021	0.06	8.95E-22	Down
Nnat	-1.38161	0.018	0.13	2.21E-112	Down
Pomc	-1.61738	0.008	0.059	3.14E-48	Down

Table 1 (continued)

Gene	log2FoldChange	pct.1	pct.2	Adjusted *p* value	up_down
Lyz1	-1.76227	0.275	0.366	2.92E-17	Down
Gh	-5.88344	0.001	0.879	0	Down
Prl	-6.15042	0	0.68	0	Down

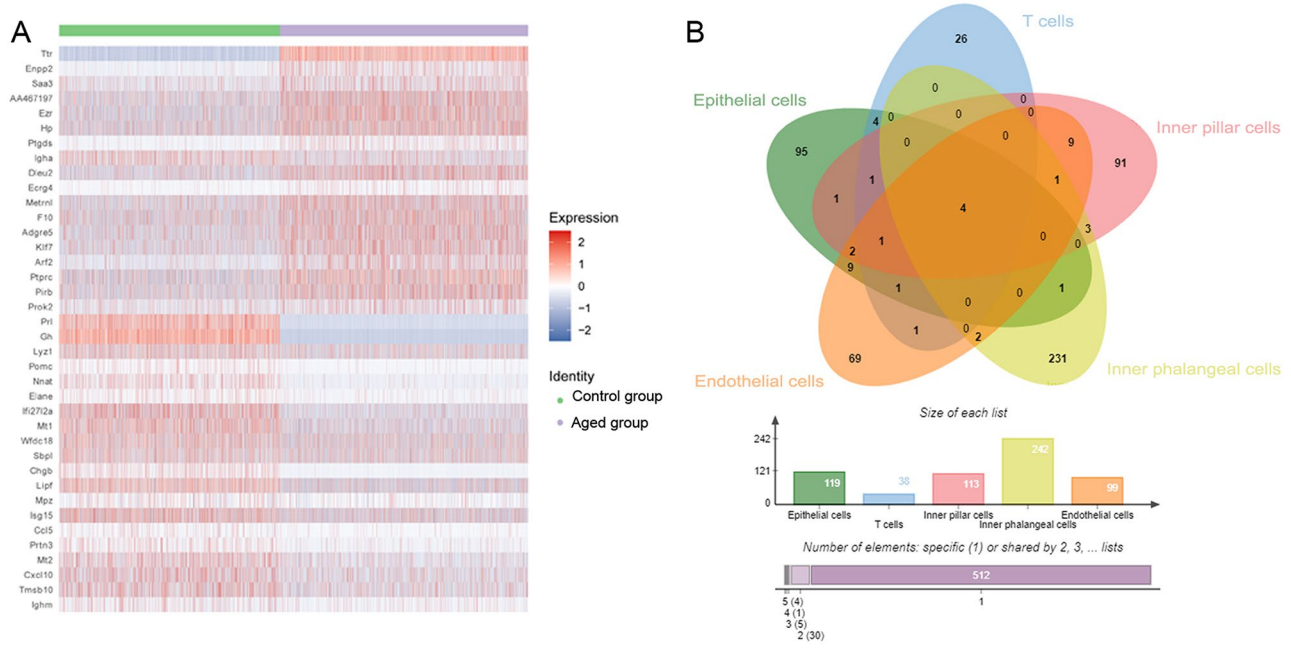

Fig. 4 Identifying the presbycusis-related genes and functional analysis. (**A**). Heatmap of top 20 genes with up-regulated or down-regulated expression in cochlear tissue. (**B**). The VENN diagram of cell-type specific DEGs

signaling pathway", the DEGs in inner phalangeal cells were significantly associated with "PI3K-Akt signaling pathway", "Oxidative phosphorylation", and "RNA transport", and the DEGs in endothelial cells were significantly associated with "Toll-like receptor signaling pathway", "Cytokine-cytokine receptor interaction" and "Rap1 signaling pathway" (Supplementary Table 3).

Immunohistochemical verification of presbycusis-related proteins

The protein expression of five DEGs, including two upregulated genes, Enpp2 and Saa3, and three down-regulated genes, Cxcl10, Ccl5 and Gh, was further verified by immunohistochemical analysis. As shown in Fig. 5, Enpp2, Cxcl10, Gh, Ccl5 and Saa3 markers can be detected in the mouse cochlea. Among them, Enpp2 and Saa3 were up-regulated in the aged mouse cochlea, while Cxcl10, Gh, and Ccl5 were down-regulated in the aged mouse cochlea.

Alterations of intercellular communication mediated by specific signaling pathways in presbycusis

To explore potential interactions among these presbycusis-related cell types, we performed CellChat analysis on the datasets. The global intercellular communication between the control and aged cochlear samples was quantified and visualized. We observed the general interaction number and interaction strength between fibroblast and other four cell types (T cell, B cell, inner phalangeal cell, and myeloid cell) were decreased in presbycusis status compared with that under healthy status (Fig. 6A and B).

We also calculated the information flow of the signal, which was defined as communication probability among the cell types. Notably, 34 out of 48 pathways were highly activated both in control and in the aged cochlea. Compared with the control group, Fn1, Galectin, Spp1, Sema3, Fgf, Calcr, Gas, and Sema6 signals were turned off. Collagen, Cd52, and Ptn signals were significantly decreased, whereas Mpz, App, and Cxcl signals were increased (Fig. 6C).

Discussion

We conducted a single-cell transcriptome sequencing study on the mice cochlear tissue from young and aged group, identified 18 distinct transcriptionally defined clusters, corresponding to 10 cell types, including myeloid cells, epithelial cells, fibroblasts, inner pillar cells

Table 2 KEGG enrichment analysis of DEGs between control and aged groups

Pathway ID	Term	*P*-value	Enrichment score	Genes
rno03010	Ribosome	5.58E-39	5.801469	Rps28; Rplp0; Rpl32; Rpl9; Rpl37a; Rpl38; Rpsa; Rpl41; Rpl19; Rps19; Rpl35a; Rps15a; Rpl36; Uba52; Rpl11; Rpl13; Rpl27a; Rpl26; Rpl34; Rps3; Rps24; Rpl30; Rpl23; Rpl14; Rps21; Rpl7a; Rps23; Rps8; Rpl17; Rpl37; Rpl28; Rps20; Rps18; Rps27a; Rpl12; Rps6; Rpl3; Rpl8; Rpl10a; Rps5; Rps4x; Rpl6; Rps27; Rplp2; Rpl29; Rpl36al; Rpl35; Rps7; Rpl18; Rpl22l1; Rpl18a; Rpl15; Rpl27; Rpl36a; Rpl5; Rps14; Rpl39; Rplp1; Rpl13a; Rps15; Rpl31; Rps11; Rpl7; Rps17; Rps29; Rps2; Rpl24; Rpl4; Rpl21; Rps12; Rps25; Rpl23a; Rps10; Rps27l; Rps16; Rpl10
rno04620	Toll-like receptor signaling pathway	0.000401	3.995148	Cxcl10; Irf7; Spp1; Ikbke; Fos; Ccl5; Map3k8; Cxcl9; Ccl4
rno05133	Pertussis	0.002322	3.811667	Rhoa; Irf1; Fos; Itgb2; C3; Nos2; Il10
rno05210	Colorectal cancer	0.002707	3.333819	Rhoa; Bcl2l11; Kras; Fos; Gadd45g; Ereg; Gadd45b; Ralgds
rno04623	Cytosolic DNA-sensing pathway	0.00282	4.224754	Zbp1; Cxcl10; Irf7; Ikbke; Ccl5; Ccl4
rno05206	MicroRNAs in cancer	0.004307	2.669234	Ezr; Marcks; Rhoa; Cd44; Zeb2; Bcl2l11; Kras; Socs1; Stmn1; Ptgs2
rno05140	Leishmaniasis	0.005798	2.943372	Ighg1; Fos; Ncf1; Itgb2; C3; Nos2; Il10; Ptgs2
rno05146	Amoebiasis	0.006731	2.663432	Gnas; Ighg1; Itgb2; Ctsg; Ighm; Nos2; Col3a1; Il10; Hspb1
rno05134	Legionellosis	0.009348	3.311293	Hspa8; Eef1g; Itgb2; Bnip3; C3; Eef1a1
rno04670	Leukocyte transendothelial migration	0.009608	2.700118	Ezr; Rhoa; Msn; Vasp; Rhoh; Rap1b; Ncf1; Itgb2
rno04210	Apoptosis	0.011812	2.43413	Bcl2l11; Kras; Fos; Cflar; Lmna; Gadd45g; Tuba1b; Gadd45b; Tuba1c
rno04062	Chemokine signaling pathway	0.014951	2.219526	Rhoa; Cxcl10; Kras; Rap1b; Ncf1; Ccl5; Fgr; Cxcl9; Hck; Ccl4
rno04668	TNF signaling pathway	0.017397	2.622706	Ifi47; Cxcl10; Fos; Cflar; Ccl5; Map3k8; Ptgs2
rno04611	Platelet activation	0.022393	2.317123	Rhoa; Vasp; Apbb1ip; Gnas; Rap1b; Ighm; Ppp1cb; Col3a1
rno04015	Rap1 signaling pathway	0.025129	1.961712	Rhoa; Vasp; Apbb1ip; Kras; Gnas; Rap1b; Itgb2; Fpr1; Prkd3; Ralgds; Flt1
rno04660	T cell receptor signaling pathway	0.026708	2.402311	Ptprc; Rhoa; Kras; Fos; Map3k8; Il10; Ctla4
rno05142	Chagas disease (American trypanosomiasis)	0.031235	2.324187	Gnas; Fos; Cflar; C3; Ccl5; Nos2; Il10
rno04657	IL-17 signaling pathway	0.035818	2.450357	Lcn2; Cxcl10; S100a9; Ikbke; Fos; Ptgs2
rno04917	Prolactin signaling pathway	0.038246	2.686795	Prl; Irf1; Kras; Socs1; Fos
rno05418	Fluid shear stress and atherosclerosis	0.038953	2.080983	Klf2; Rhoa; Nfe2l2; Mef2a; Fos; Sumo2; Ncf1; Sdc4

and inner phalangeal cells. Cellchat analysis revealed the intercellular communications of several cell types were greatly altered in presbycusis status, and specific signaling pathways changed were also observed, such as collagen, Cd52, and Cxcl signals. Moreover, numerous DEGs were screened from aged cochlear tissue, and these genes were mainly involved in immune, oxidative stress, apoptosis, and metabolic processes. Immunohistochemistry verification showed five (Enpp2, Cxcl10, Gh, Ccl5, and Saa3) markers could be detected in the mouse cochlea and displayed a significant differential expression in presbycusis.

Among these molecules, ectonucleotide pyrophosphatase/phosphodiesterase family member 2 (ENPP2) is ubiquitously expressed in human tissues, and plays a key role in the production of extracellular lysophosphatidic acid [21]. It is closely related to both senile diseases [22] and erastin-induced ferroptosis [23]. Here, we found ENPP2 was significantly up-regulated in the cochlea of presbycusis mice. Functional enrichment shows that ENPP2 is mainly involved in ferroptosis-related processes such as ion metabolism, lipid decomposition, and metabolism. Thus, we speculate that ENPP2 may be critically involved in the human presbycusis by regulating ferroptosis.

CCL5 encodes a protein of RANTES, which is a member of the chemokine family and serves a crucial role in inflammation and immune responses [24]. Previous studies have determined that CCL5 was involved in the human deafness via multiple pathways. For example, CCL5 may directly regulate the occurrence of noise-induced deafness through inducing cochlear oxidative stress [25]. The infiltration of CCL5 in eosinophilic otitis media (EOM) is significantly increased [26]. In our study, the expression of CCL5 mRNA is also deregulated in the cochlear sample of aged group, which is in accordance with its protein expression pattern detected by immunohistochemistry.

CXCL10 belongs to non-ELR subfamily. It is a class of chemokine induced by interferon-gamma that can chemotactic a variety of immune cells such as monocyte, T lymphocyte, and natural killer cell. CXCL10 regulates

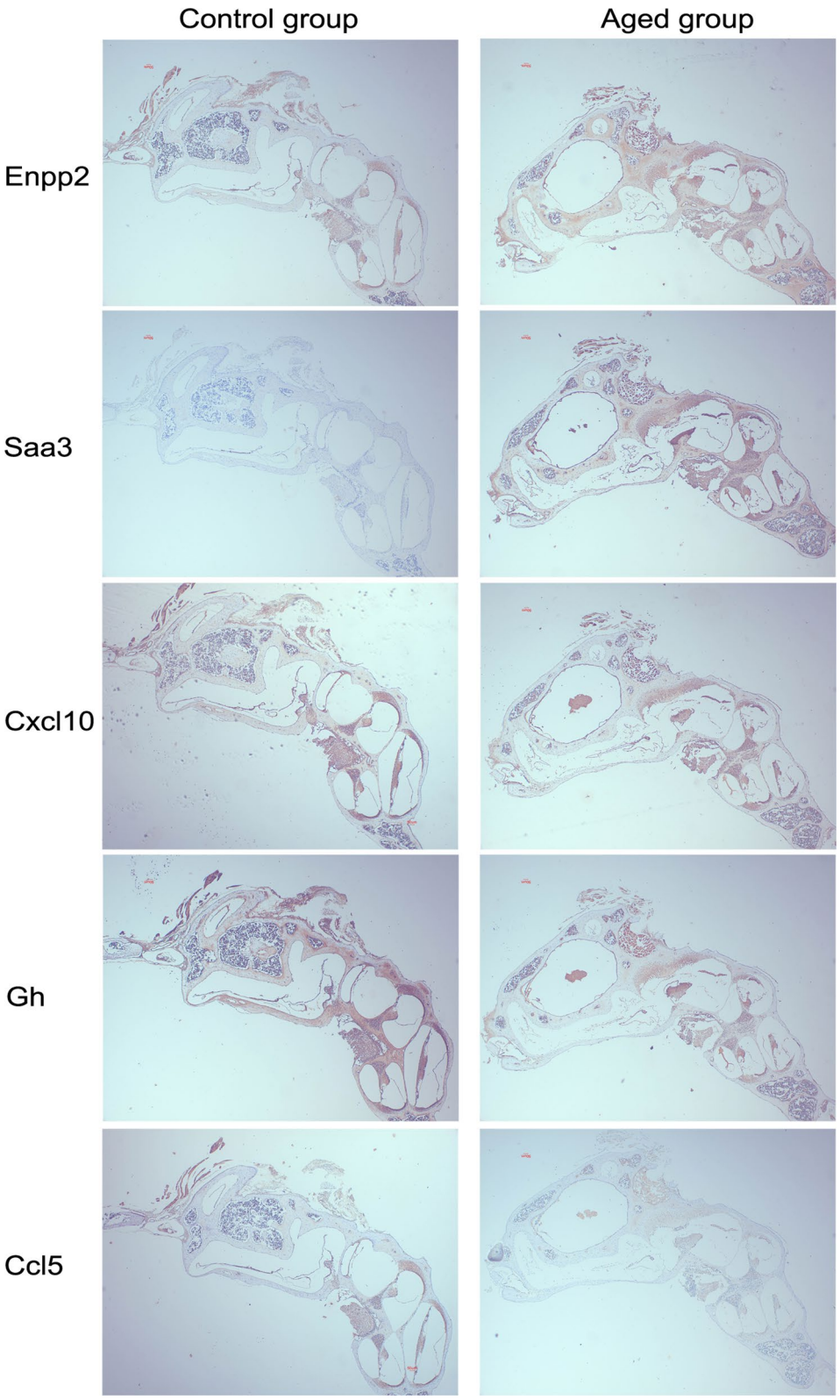

Fig. 5 Immunohistochemical verification for crucial molecules related to presbycusis. Five biological replicates of the whole cochlear tissues in each group were performed for each protein. The representative images for each protein are displayed

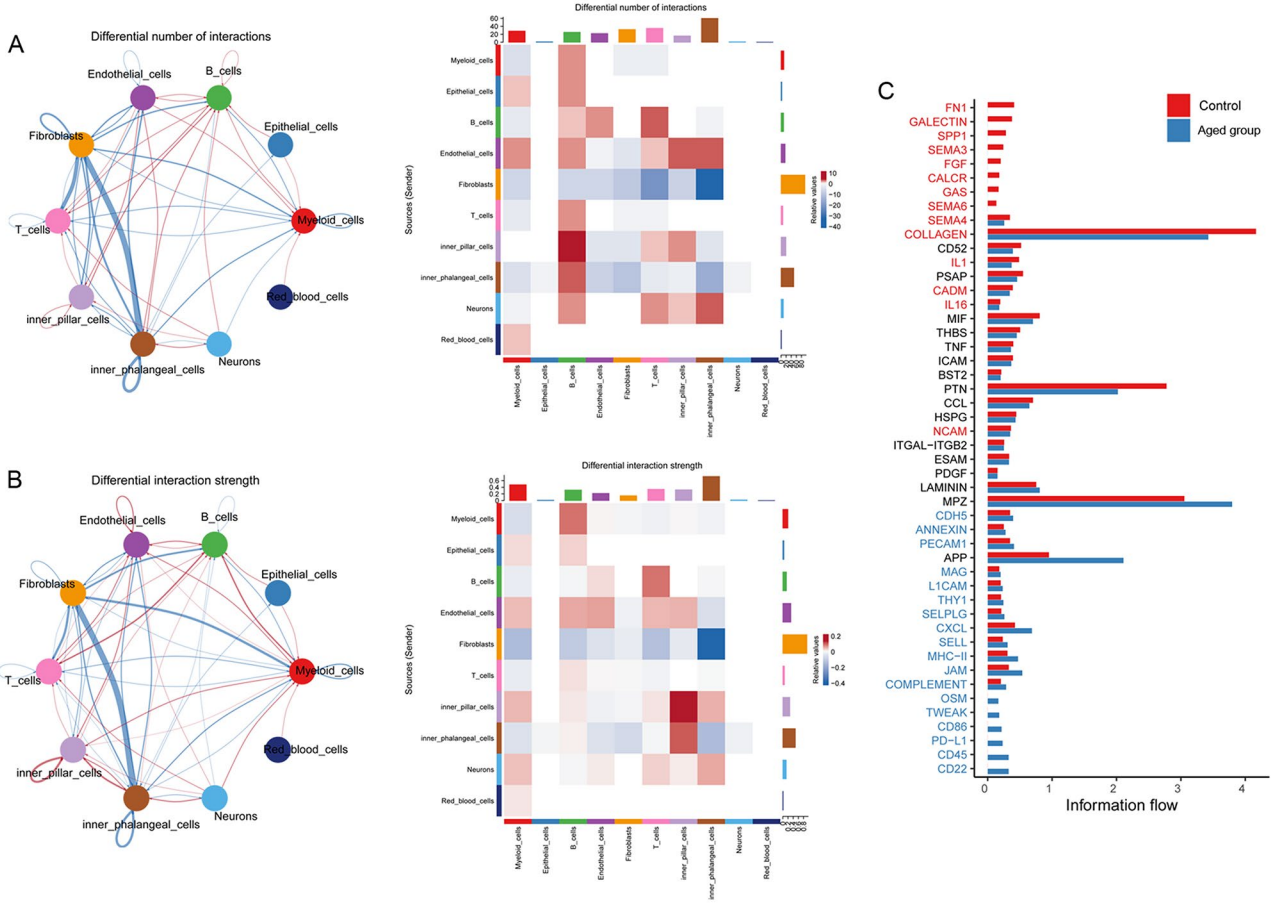

Fig. 6 Analysis of cellular communication by CellChat displayed the alterations of several pathways in normal and presbycusis. (**A**-**B**). Circle plots (left side) and heatmaps (right side) of interaction number and interaction strength among differential cell types. Blue lines or columns represented the communication decreased in disease condition, whereas red lines or columns indicate the communication increased compared with control. (**C**). Differences in overall information flow of the signaling pathways between control and aged presbycusis samples

inflammatory responses via binding to the specific chemokine receptor CXCR3. The expression of CXCL10 is up-regulated in the presbycusis patients serum, suggesting that immune related gene CXCL10 plays an important role in the presbycusis occurrence [27].

Growth hormone (GH) is an anterior pituitary hormone secreted by the anterior pituitary gland. GH can affect the metabolism of sugar, protein and lipid in animals, as well as reproduction and immunity. GH is supposed to take part in the embryonic auditory development. GH deficiency led to hearing loss and central auditory process dysfunction. Furthermore, GH can stimulate the hair cells proliferation and synaptic transmission recovery after cochlear injury. Exogenous factors (noise, drugs or trauma) induce the GH releasing and activate downstream mediators to exert protective effects for the auditory pathways [28]. Here our data reveal the evident decrease of GH in the aged cochlea, which may be responsible for auditory transmission in presbycusis. Additionally, serum amyloid A (SAA) are evolutionary-conserved acute phase proteins in response to inflammation. The broad biological effects of SAA3 have been attributed to leukocyte recruitment, production of chemokines and MMPs [29]. There are few studies on the relationship between SAA3 and deafness.

The intercellular communications among differential cell types were analyzed and compared between two groups of cochleae. Here, we focused on those greatly altered signaling pathways in disease conditions, such as Collagen, Cd52, Ptn, Mpz, App, and Cxcl. For details, the hub of the Collagen signal is fibroblasts, and the outgoing signal to other cell types was significantly reduced in presbycusis (Supplementary Fig. 2). Collagen is the essential constituent of extracellular matrix (ECM), which plays an vital role in the structure maintaining of inner ear [30]. The expression of multiple collagen types (I-V, IX, and XI) has been detected in the inner ear [31, 32]. The mice lacking DDR1, a main class of collagen-binding receptor, displayed inner ear defects and hearing loss [30]. Collagen changes in the aged rats cochlea were also revealed, and the collagen fibers were markedly decreased in the inner ear area of connecting spiral

ligament and stria vascular [33]. A recent study showed collagen proteins abundance were significant decreased in loud noise-induced hearing loss; the potential mechanisms were associated with proteotoxic stress and proteostasis network activation [34]. Considering this, we suggested that fibroblasts crosstalk with inner phalangeal cell and myeloid cell via collagen signaling in presbycusis.

Some limitations remain existed in our study. Firstly, the number of cochlear tissues used for single cell sequencing was small in this study. Due to limitation of fund, only one biological replicate was used for each age group. A notable finding of our study was that myeloid cells constitute the predominant cell population of samples in both young and aged groups. Besides, we noticed the counts of epithelial cells, inner pillar cells, inner phalangeal cells, T and B cells were decreased in the cochlear tissues of aged mice, while the counts of endothelial cells, neurons, fibrocytes, and red blood cells were increased in the aged samples. The abundance of immune cells might because that the tissues used in the single cell sequencing included the bony shell of the cochlea, which contains a significant amount of bone marrow immune cells. However, these discrepancies warrant thorough confirmation with an additional observation using histology or flow cytometry since only one biological replicate was used. Second, due to the known technological difficulties associated with isolating mature neurons with intact dendrites and axons as well as the scarcity in the number of HCs, we only captured a small number of spiral ganglion neurons and HCs were not clustered and we could not assess the crosstalk effect between HCs and other cell types. Therefore, more samples across multiple developmental time points should be acquired for the cell type's specific changes detection.

In this study, we established a cell-type-specific transcriptome profile of the cochlea of aged mice, and verified significantly DEGs by immunohistochemical assay. In addition, we performed pathway analysis to identify the underlying mechanisms by which presbycusis occurs. The completion of this study promoted new ideas for further revealing the pathogenesis of presbycusis, and provided novel potential targets for the development of therapeutic drugs.

Abbreviations

ARHL	Age-related hearing loss
DEGs	Differentially expressed genes
scRNA-seq	Hair cells (HCs); single-cell sequencing
ABR	Auditory brainstem response
SPL	Sound pressure level
EDTA	Ethylenediaminetetraacetic acid
SDs	Standard deviations
UMI	Unique molecular identifier
PCA	Principal component analysis
tSNE	t-distributed stochastic neighbor embedding
GO	Gene ontology
KEGG	Kyoto Encyclopedia of Genes and Genomes
ENPP2	Ectonucleotide pyrophosphatase/phosphodiesterase family member 2
ENPP2	Ectonucleotide pyrophosphatase/phosphodiesterase family member 2
GH	Growth hormone
SAA	Serum amyloid A
ECM	Extracellular matrix

Supplementary Information

The online version contains supplementary material available at https://doi.org/10.1186/s12920-024-02001-7.

Supplementary Material 1

Supplementary Material 2

Supplementary Material 3

Supplementary Material 4

Supplementary Material 5

Acknowledgements
Not applicable.

Author contributions
JZ carried out the conception and design of the research, JZ, WS, YL, SK and WY participated in the acquisition of data. MF and ZC carried out the analysis and interpretation of data. HLM and HZM performed the statistical analysis. JZ and SK drafted the manuscript. YH, JG, YJL, LLX and WY revised the manuscript for important intellectual content. All authors read and approved the final manuscript.

Funding
This study was supported by the Young and middle-aged medical high-end talents in Chongqing (The 7th batch), Chongqing medical scientific research general project (Joint project of Chongqing Health Commission and Science and Technology Bureau) (No. cstc2021jcyj-bshX0026), Chongqing Technology innovation and application development special project (No. CSTB2023TIAD-KPX0059), Chongqing young and middle-aged medical excellence team (The 1st batch), Chongqing Talent Program. Innovative leading talents in the medical field (2021), Chongqing medical scientific research major project (Joint project of Chongqing Health Commission and Science and Technology Bureau) (No. 2022DBXM006) and General Program of Chongqing Natural Science Foundation (No. cstc2021jcyj-msxmX0128).

Data availability
The datasets generated during the current study are available from the NCBI SRA database with accession number of PRJNA1013607.

Declarations

Ethics approval and consent to participate
All animal experiments were reported in accordance with ARRIVE guidelines and the experimental procedures were approved by the Laboratory Animal Welfare and Ethics Committee of the Third Military Medical University (ID: IACUC-CQMU-2022-0030).

Consent for publication
Not applicable.

Competing interests
The authors declare no competing interests.

Received: 31 July 2023 / Accepted: 29 August 2024
Published online: 30 September 2024

References

1. Collaborators GHL. Hearing loss prevalence and years lived with disability, 1990–2019: findings from the global burden of Disease Study 2019. Lancet. 2021;397(10278):996–1009.
2. Chester J, Johnston E, Walker D, Jones M, Ionescu CM, Wagle SR, Kovacevic B, Brown D, Mikov M, Mooranian A, Al-Salami H. A Review on Recent Advancement on Age-Related Hearing Loss: The Applications of Nanotechnology, Drug Pharmacology, and Biotechnology. *Pharmaceutics* 2021, 13(7).
3. Brewster KK, Hu MC, Zilcha-Mano S, Stein A, Brown PJ, Wall MM, Roose SP, Golub JS, Rutherford BR. Age-related hearing loss, late-life Depression, and risk for Incident Dementia in older adults. J Gerontol Biol Sci Med Sci. 2021;76(5):827–34.
4. Yue T, Chen Y, Zheng Q, Xu Z, Wang W, Ni G. Screening tools and Assessment methods of Cognitive decline Associated with Age-related hearing loss: a review. Front Aging Neurosci 2021, 13(677090).
5. Deng T, Li J, Liu J, Xu F, Liu X, Mi J, Bergquist J, Wang H, Yang C, Lu L et al. Hippocampal Transcriptome-Wide Association Study Reveals Correlations Between Impaired Glutamatergic Synapse Pathway and Age-Related Hearing Loss in BXD-Recombinant Inbred Mice. *Front Neurosci* 2021, 15(745668).
6. Xue N, Song L, Song Q, Santos-Sacchi J, Wu H, Navaratnam D. Genes related to SNPs identified by genome-wide association studies of age-related hearing loss show restriction to specific cell types in the adult mouse cochlea. Hear Res. 2021;410(108347):4.
7. Kim YJ, Choo OS, Lee JS, Jang JH, Woo HG, Choung YH. BCL2 interacting protein 3-like/NIX-mediated Mitophagy plays an important role in the process of Age-related hearing loss. Neuroscience. 2021;455:39–51.
8. Rivas-Chacón LDM, Martínez-Rodríguez S, Madrid-García R, Yanes-Díaz J, Riestra-Ayora JI, Sanz-Fernández R, Sánchez-Rodríguez C. Role of oxidative stress in the Senescence Pattern of Auditory cells in age-related hearing loss. Antioxidants 2021, 10(9).
9. Iwai H, Inaba M, Van Bui D, Suzuki K, Sakagami T, Yun Y, Mitani A, Kobayashi Y, Kanda A. Treg and IL-1 receptor type 2-expressing CD4(+) T cell-deleted CD4(+) T cell fraction prevents the progression of age-related hearing loss in a mouse model. J Neuroimmunol. 2021;357(577628):8.
10. Liu Y, Wei M, Mao X, Chen T, Lin P, Wang W. Key Signaling Pathways Regulate the Development and Survival of Auditory Hair Cells. *Neural Plast* 2021, 11(5522717).
11. Kolla L, Kelly MC, Mann ZF, Anaya-Rocha A, Ellis K, Lemons A, Palermo AT, So KS, Mays JC, Orvis J, et al. Characterization of the development of the mouse cochlear epithelium at the single cell level. Nat Commun. 2020;11(1):020–16113.
12. Ranum PT, Goodwin AT, Yoshimura H, Kolbe DL, Walls WD, Koh JY, He DZZ, Smith RJH. Insights into the Biology of hearing and Deafness revealed by single-cell RNA sequencing. Cell Rep. 2019;26(11):3160–71.
13. Jin S, Guerrero-Juarez CF, Zhang L, Chang I, Ramos R, Kuan CH, Myung P, Plikus MV, Nie Q. Inference and analysis of cell-cell communication using CellChat. Nat Commun. 2021;12(1):021–21246.
14. Su Z, Xiong H, Pang J, Lin H, Lai L, Zhang H, Zhang W, Zheng Y. LncRNA AW112010 promotes mitochondrial Biogenesis and Hair Cell Survival: implications for age-related hearing loss. Oxid Med Cell Longev 2019, 27(6150148).
15. McGinnis CS, Murrow LM, Gartner ZJ. DoubletFinder: Doublet Detection in single-cell RNA sequencing data using Artificial Nearest neighbors. Cell Syst. 2019;8(4):329–37.
16. Butler A, Hoffman P, Smibert P, Papalexi E, Satija R. Integrating single-cell transcriptomic data across different conditions, technologies, and species. Nat Biotechnol. 2018;36(5):411–20.
17. Aran D, Looney AP, Liu L, Wu E, Fong V, Hsu A, Chak S, Naikawadi RP, Wolters PJ, Abate AR, et al. Reference-based analysis of lung single-cell sequencing reveals a transitional profibrotic macrophage. Nat Immunol. 2019;20(2):163–72.
18. Zhao Y, Zhang Q, Tu K, Chen Y, Peng Y, Ni Y, Zhu G, Cheng C, Li Y, Xiao X, et al. Single-cell transcriptomics of Immune cells reveal diversity and exhaustion signatures in Non-small-cell Lung Cancer. Front Immunol. 2022;13:854724.
19. Schlesinger Y, Yosefov-Levi O, Kolodkin-Gal D, Granit RZ, Peters L, Kalifa R, Xia L, Nasereddin A, Shiff I, Amran O, et al. Single-cell transcriptomes of pancreatic preinvasive lesions and cancer reveal acinar metaplastic cells' heterogeneity. Nat Commun. 2020;11(1):4516.
20. Chen YP, Yin JH, Li WF, Li HJ, Chen DP, Zhang CJ, Lv JW, Wang YQ, Li XM, Li JY, et al. Single-cell transcriptomics reveals regulators underlying immune cell diversity and immune subtypes associated with prognosis in nasopharyngeal carcinoma. Cell Res. 2020;30(11):1024–42.
21. Reeves VL, Trybula JS, Wills RC, Goodpaster BH, Dubé JJ, Kienesberger PC, Kershaw EE. Serum Autotaxin/ENPP2 correlates with insulin resistance in older humans with obesity. Obesity. 2015;23(12):2371–6.
22. Ramesh S, Govindarajulu M, Suppiramaniam V, Moore T, Dhanasekaran M. Autotaxin¯Lysophosphatidic Acid Signaling in Alzheimer's Disease. Int J Mol Sci 2018, 19(7).
23. Bai YT, Chang R, Wang H, Xiao FJ, Ge RL, Wang LS. ENPP2 protects cardiomyocytes from erastin-induced ferroptosis. Biochem Biophys Res Commun. 2018;499(1):44–51.
24. Marques RE, Guabiraba R, Russo RC, Teixeira MM. Targeting CCL5 in inflammation. Expert Opin Ther Targets. 2013;17(12):1439–60.
25. Jamesdaniel S, Rosati R, Westrick J, Ruden DM. Chronic lead exposure induces cochlear oxidative stress and potentiates noise-induced hearing loss. Toxicol Lett. 2018;292:175–80.
26. Kudo N, Matsubara A, Nishizawa H, Miura T. Immunohistological analysis of eotaxin and RANTES in the model animal of eosinophilic otitis media. Acta Otolaryngol. 2017;137(5):476–81.
27. Dong Y, Li M, Liu P, Song H, Zhao Y, Shi J. Genes involved in immunity and apoptosis are associated with human presbycusis based on microarray analysis. Acta Otolaryngol. 2014;134(6):601–8.
28. Gómez JG, Devesa J. Growth hormone and the auditory pathway: Neuromodulation and Neuroregeneration. Int J Mol Sci 2021, 22(6).
29. Abouelasrar Salama S, De Bondt M, Berghmans N, Gouwy M, de Oliveira VLS, Oliveira SC, Amaral FA, Proost P, Van Damme J, Struyf S, De Buck M. Biological Characterization of Commercial Recombinantly Expressed Immunomodulating Proteins Contaminated with Bacterial Products in the Year 2020: The SAA3 Case. *Mediators Inflamm* 2020, 6(6087109).
30. Meyer zum Gottesberge AM, Gross O, Becker-Lendzian U, Massing T, Vogel WF. Inner ear defects and hearing loss in mice lacking the collagen receptor DDR1. Lab Invest. 2008;88(1):27–37.
31. Asamura K, Abe S, Imamura Y, Aszodi A, Suzuki N, Hashimoto S, Takumi Y, Hayashi T, Fässler R, Nakamura Y, Usami S. Type IX collagen is crucial for normal hearing. Neuroscience. 2005;132(2):493–500.
32. Cosgrove D, Samuelson G, Pinnt J. Immunohistochemical localization of basement membrane collagens and associated proteins in the murine cochlea. Hear Res. 1996;97(1–2):54–65.
33. Buckiova D, Popelar J, Syka J. Collagen changes in the cochlea of aged Fischer 344 rats. Exp Gerontol. 2006;41(3):296–302.
34. Jongkamonwiwat N, Ramirez MA, Edassery S, Wong ACY, Yu J, Abbott T, Pak K, Ryan AF, Savas JN. Noise exposures causing hearing loss generate proteotoxic stress and activate the Proteostasis Network. Cell Rep. 2020;33(8):108431.

Publisher's note